Sequential and recyclable sensing of Fe^{3+} and ascorbic acid in water with a terbium(III)-based metal−organic framework

Ke-Yang Wu, Liang Qin, Cheng Fan, Shao-Lan Cai, Ting-Ting Zhang,

Wen-Hua Chen, Xiao-Yan Tang* and Jin-Xiang Chen*

Table S1 Crystallographic data for MOF **1**.

Molecular formula	$C_{18}H_{32}N_4O_{29}Tb_2$	D_{calc} (g cm^{-3})	2.239
Formula weight	1086.31	λ (Mo-Kα) (Å)	0.71073
Crystal system	monoclinic	μ (cm^{-1})	4.475
Space group	$P2_1/n$	Total reflections	18195
a (Å)	10.1266(8)	Unique reflections	3709
b (Å)	15.5118(13)	No. observations	3437
c (Å)	10.4954(9)	No. parameters	250
α (°)	90	R^a	0.0229
β (°)	102.2370(10)	wR^b	0.0442
γ (°)	90	GOF^c	1.137
V (Å^3)	1611.2 (2)	$\Delta\rho_{max}$ (e Å^{-3})	0.622
Z	2	$\Delta\rho_{min}$ (e Å^{-3})	−1.067
T/K	296(2)		

^{a} $R_1 = \Sigma||F_o| - |F_c|/\Sigma|F_o||$. ^{b} $wR_2 = \{\Sigma[w(F_o^2 - F_c^2)^2/\Sigma w(F_o^2)^2]\}^{1/2}$. ^{c} GOF $= \{\Sigma[w((F_o^2 - F_c^2)^2)/(n - p)\}^{1/2}$, where n = number of reflections and p = total numbers of parameters refined.

Table S2 Selected bond distances (Å) and angles (º) for MOF **1**.

Tb(1)-O(1)	2.3559(16)	Tb(1)-O(3)#2	2.5547(17)
Tb(1)-O(1W)	2.4622(17)	Tb(1)-O(4)#2	2.5238(16)
Tb(1)-O(2W)	2.4391(16)	Tb(1)-O(5)#3	2.3953(16)
Tb(1)-O(2)#1	2.3456(16)	Tb(1)-O(6)#4	2.3697(16)
Tb(1)-O(3W)	2.4714(16)		
O(1)-Tb(1)-O(1W)	139.83(6)	O(6)#4-Tb(1)-O(2W)	142.13(6)
O(1)-Tb(1)-O(2W)	140.41(6)	O(6)#4-Tb(1)-O(3W)	136.09(6)
O(1)-Tb(1)-O(3W)	67.45(6)	O(6)#4-Tb(1)-O(3)#2	115.96(6)
O(1)-Tb(1)-O(3)#2	116.26(5)	O(6)#4-Tb(1)-O(4)#2	75.48(6)
O(1)-Tb(1)-O(4)#2	76.50(6)	O(6)#4-Tb(1)-O(5)#3	118.79(6)
O(1)-Tb(1)-O(5)#3	76.58(6)	O(6)#4-Tb(1)-C(9)#2	96.73(6)
O(1)-Tb(1)-O(6)#4	74.62(6)	O(6)#4-Tb(1)-O(5)#3	118.79(6)
O(1)-Tb(1)-C(9)#2	95.94(6)	O(6)#4-Tb(1)-C(9)#2	96.73(6)
O(1W)-Tb(1)-O(3W)	130.96(6)	O(2)#1-Tb(1)-O(6)#4	74.83(6)
O(1W)-Tb(1)-O(3)#2	65.14(6)	O(2)#1-Tb(1)-C(9)#2	141.20(6)
O(1W)-Tb(1)-O(4)#2	76.26(6)	O(3W)-Tb(1)-O(3)#2	65.85(6)
O(1W)-Tb(1)-C(9)#2	69.78(6)	O(3W)-Tb(1)-O(4)#2	74.90(6)
O(2W)-Tb(1)-O(1W)	79.22(6)	O(3W)-Tb(1)-C(9)#2	66.98(6)
O(2W)-Tb(1)-O(3W)	81.21(6)	O(3)#2-Tb(1)-C(9)#2	25.64(5)
O(2W)-Tb(1)-O(3)#2	67.64(5)	O(4)#2-Tb(1)-O(3)#2	51.32(5)
O(2W)-Tb(1)-O(4)#2	118.95(5)	O(4)#2-Tb(1)-C(9)#2	25.74(6)
O(2W)-Tb(1)-C(9)#2	93.24(6)	O(5)#3-Tb(1)-O(1W)	138.37(6)
O(2)#1-Tb(1)-O(1)	117.07(6)	O(5)#3-Tb(1)-O(2W)	71.50(6)
O(2)#1-Tb(1)-O(1W)	71.76(6)	O(5)#3-Tb(1)-O(3W)	73.26(6)
O(2)#1-Tb(1)-O(2W)	74.62(6)	O(5)#3-Tb(1)-O(3)#2	125.16(6)
O(2)#1-Tb(1)-O(3W)	142.71(6)	O(5)#3-Tb(1)-O(4)#2	144.23(6)
O(2)#1-Tb(1)-O(3)#2	126.47(6)	O(5)#3-Tb(1)-C(9)#2	139.18(6)
O(2)#1-Tb(1)-O(4)#2	141.99(6)	O(6)#4-Tb(1)-O(1W)	70.35(6)
O(2)#1-Tb(1)-O(5)#3	72.36(6)		

Symmetry transformations used to generate equivalent atoms: #1 $-x + 1, -y - 2, -z + 1$; #2 $x - 1/2, -y - 3/2, z + 1/2$; #3 $-x + 3/2, y - 1/2, -z + 3/2$; #4 $x - 1/2, -y - 3/2, z - 1/2$; #5 $x + 1/2, -y - 3/2, z - 1/2$; #6 $-x + 3/2, y + 1/2, -z + 3/2$; #7 $x + 1/2, -y - 3/2, z + 1/2$.

Table S3 Comparison of the detection limit in MOF–based luminescent sensors for the detection of Fe^{3+} and ascorbic acid.

Analyte	MOF	Detection limit (μM)	Ref.
Fe^{3+}	$[Zr_6O_4(OH)_4(2,7\text{-}CDC)_6]\cdot 19H_2O\cdot 2DMF$	0.91	1
Fe^{3+}	$\{[Eu_2L_{1.5}(H_2O)_2EtOH]\cdot DMF\}_n$	10	2
Fe^{3+}	$[Tb(TBOT)(H_2O)](H_2O)_4(DMF)(NMP)_{0.5}$	130	3
Fe^{3+}	$[(CH_3)_2NH_2]\cdot[Tb(bptc)]\cdot$xsolvents	180	4
Fe^{3+}	MOF **1**	4.0	This work
AA	Tb-CP	0.2	5
AA	$[UO_2(L)DMA]_n$	21.53	6
AA	$[\{(H_3O)[Eu(SBDB)(H_2O)_2]\}_n]$	5.0	7
AA	ZJU-136-$Ce_{1-x}Eu_x$ (x = 0.24, 0.36)	12.6	8
AA	MOF **1**	5.9	This work

2,7-CDC = 9H-carbazole-2,7-dicarboxylate
L = 5,5'-(carbonylbis(azanediyl))diisophthalic acid
NMP = N-methyl-2-pyrrolidone
bptc = biphenyl-3,3',5,5'-tetracarboxylate
L = [6-(carboxymethyl-amino)-4-oxo-4,5-dihydro-[1,3,5]triazin-2-ylamino]-acetateAA
DMA = Dimethylacetamide
SBDB = 1,5-disulfo-benzene-2,4-dicarboxylicate

Table S4 The recovery determination of Fe^{3+} and AA in urine and serum by the standard addition method.

	Samples	*Spiked amount (mM)*	*Found amount (mM)*	*Recovery (%)*	*RSD (%, n=3)*
Fe^{3+}	Urine	0.1	0.105 ± 0.001	105.0	0.95
		0.5	0.516 ± 0.008	103.2	1.55
		1.0	0.973 ± 0.013	97.3	1.34
	Serum	0.1	0.101 ± 0.002	101.0	1.98
		0.5	0.476 ± 0.006	95.2	1.26
		1.0	0.996 ± 0.011	99.6	1.10
AA	Urine	0.25	0.240 ± 0.007	95.8	2.92
		0.75	0.787 ± 0.013	104.9	1.65
		1.25	1.266 ± 0.011	101.3	0.87
	Serum	0.25	0.257 ± 0.005	102.7	1.95
		0.75	0.740 ± 0.009	98.6	1.22
		1.25	1.301 ± 0.026	104.1	2.00

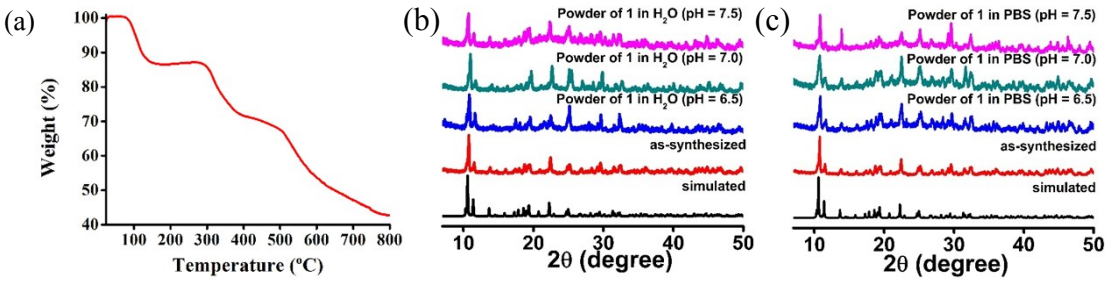

Figure S1. Thermal gravimetric analysis of MOF **1** (a). PXRD patterns of MOF **1** showing agreement with simulated, as-synthesized and MOF **1** after immersing in H_2O (b) and PBS (c) for 48 h at pH 6.5, 7.0 and 7.5.

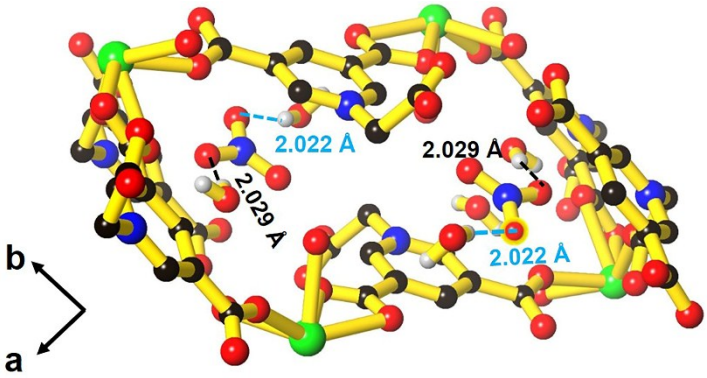

Figure S2. The pore structure of MOF **1** showing the hydrogen bonding interaction between NO_3^- and free waters. Color codes: Tb green, O red, N blue, C black, H silver grey.

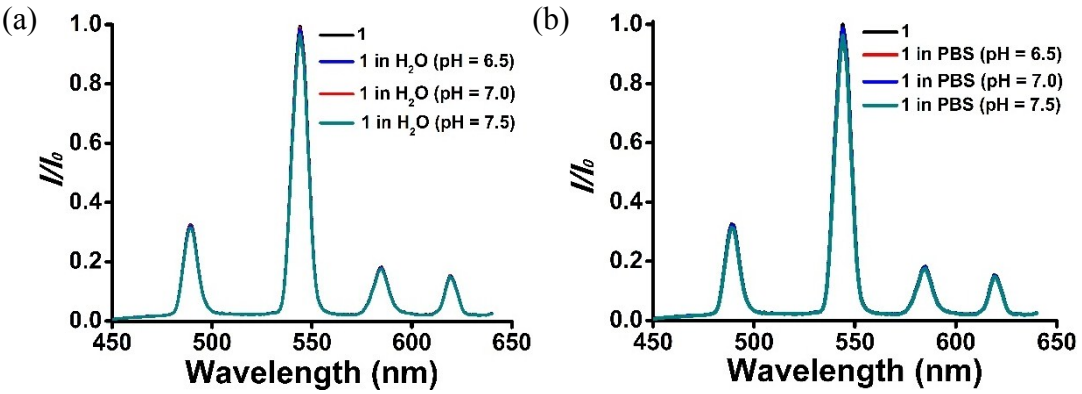

Figure S3 The Fluorescence emission spectrum of **1** in water (a) and (b) PBS with different pH environments.

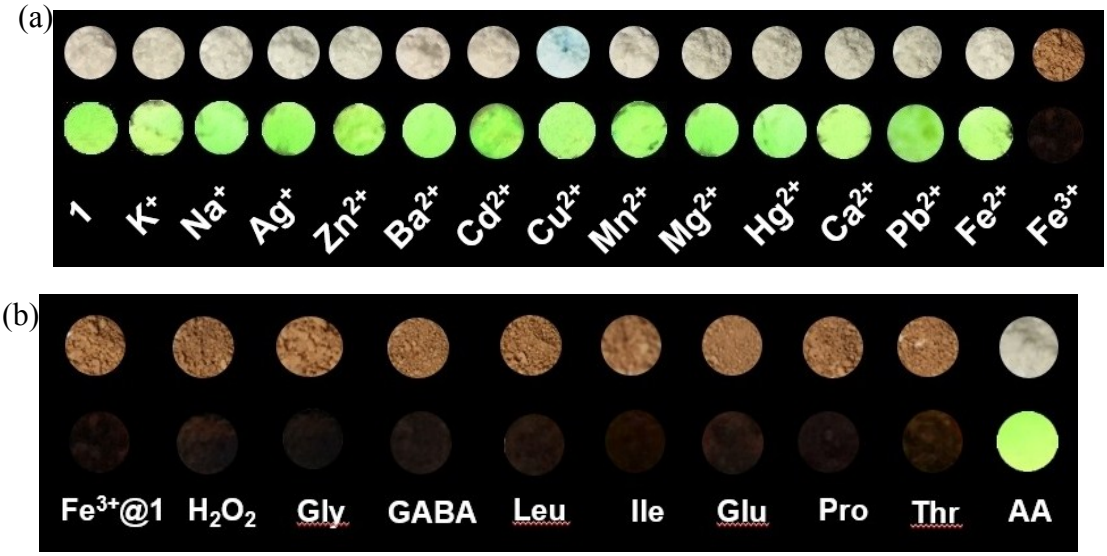

Figure S4. (a) The emission of MOF **1** seen by the naked eyes under the existence of different metal ions with natural light (up) or UV light (365 nm, down). (b) The emission of Fe^{3+}@**1** seen by the naked eyes under the existence of different substances with natural light (up) or UV light (365 nm, down).

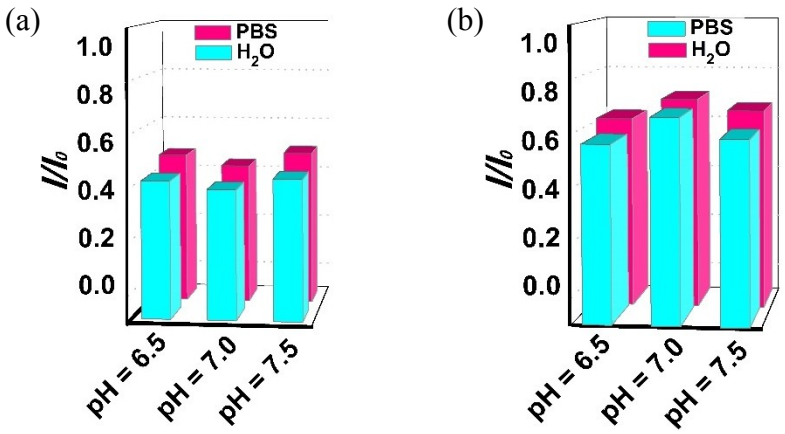

Figure S5 (a) The detection of Fe^{3+} (0.2 mM) by **1** and (b) AA (1.0 mM) by Fe^{3+}@**1** in water and PBS with different pH.

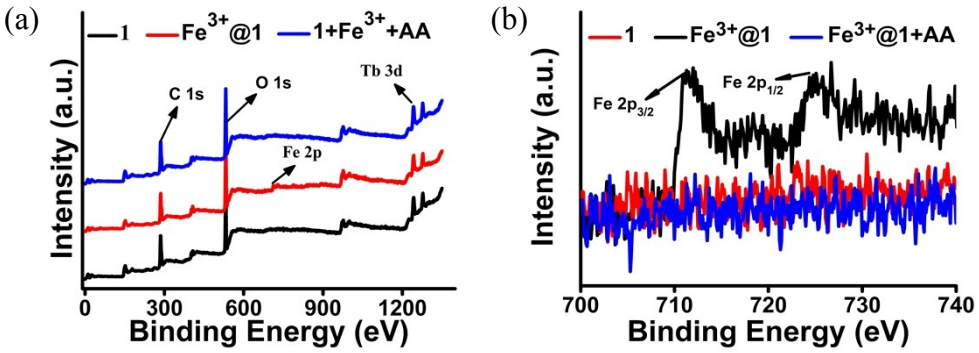

Figure S6. (a) XPS spectra for **1**, Fe^{3+}@**1** and Fe^{3+}@**1** + AA. (b) XPS for Fe $2p_{3/2}$ and Fe $2p_{1/2}$ in **1**, Fe^{3+}@**1** and Fe^{3+}@**1** + AA.

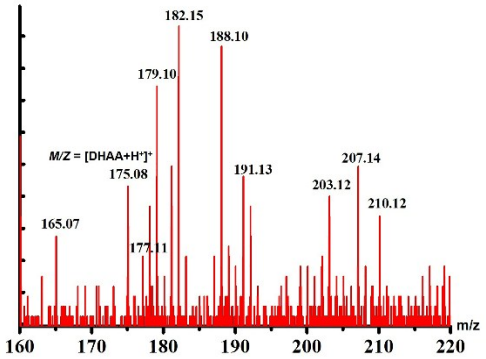

Figure S7. Electrospray ionization mass spectra for supernatant of Fe^{3+}@**1** + AA (positive), indicating the formation of dehydroascorbic acid (DHAA).

References

1. A. Das and S. Biswas, *Sens. Actuators B*, 2017, **250**, 121–131.
2. W. Liu, X. Huang, C. Xu, C. Chen, L. Yang, W. Dou, W. Chen, H. Yang and W. Liu, *Chem. Eur. J.*, 2016, **22**, 18769–18776.
3. M. Chen, W. Xu, J. Tian, H. Cui, J. Zhang, C. Liu and M. Du, *J. Mater. Chem. C*, 2017, **5**, 2015–2021.
4. X. Zhao, D. Tian, Q. Gao, H. Sun, J. Xu and X. Bu, *Dalton Trans.*, 2016, **45**, 1040–1046.
5. H. Tan, J. Wu and Y. Chen, *Microchim. Acta*, 2014, **181**, 1431–1437.
6. H. H. Tian, L. T. Chen, R. L. Zhang, J. S. Zhao, C. Y. Liu and N. S. Weng, *J. Solid State Chem.*, 2018, **258**, 674–681.
7. Y. Y. Yuan, S. L. Yang, C. X. Zhang and Q. L. Wang, *CrystEngComm*, 2018, **20**, 6989–6994.
8. D. Yue, Y. Huang, L. Zhang, K. Jiang, X. Zhang, Y. Cui, Y. Yu and G. Qian, *J. Mater. Chem. C*, 2018, **6**, 2054–2059.